Numerical Study of Heat Transfer Enhancement in Heat Exchanger Using AL_2O_3 Nanofluids

Hussein Talal Dhaiban
Assist Lecturer
Refrigeration and Air-Conditioning Tech. - Dijlah University College
husseinayo@gmail.com

ABSTRACT

In this study, the flow and heat transfer characteristics of Al_2O_3-water nanofluids for a range of the Reynolds number of 3000, 4500, 6000 and 7500 with a range of volume concentration of 1%, 2%, 3% and 4% are studied numerically. The test rig consists of cold liquid loop, hot liquid loop and the test section which is counter flow double pipe heat exchanger with 1m length. The inner tube is made of smooth copper with diameter of 15mm. The outer tube is made of smooth copper with diameter of 50mm. The hot liquid flows through the outer tube and the cold liquid (or nanofluid) flow through the inner tube. The boundary condition of this study is thermally insulated the outer wall with uniform velocity at (0.2, 0.3, 0.4 and 0.5 m/s) at the cold loop and constant velocity at (0.5 m/s) at the hot loop.

The results show that the heat transfer coefficient and Nusselt number increased by increasing Reynolds number and particle concentration. Numerical results indicate that the maximum enhancement in Nusselt number and heat transfer coefficient were 9.5% and 13.5% respectively at Reynolds number of 7100 and particles volume fraction of 4%. Results of nanofluids also showed a good agreement with the available empirical correlation at particles volume fractions of 1%, 2% and 3%, but at volume fractions of 4% a slight deviation is obtained.

Keywords: heat transfer, heat exchanger, nanofluids.

دراسة عددية لتحسين انتقال الحرارة داخل مبادل حراري باستخدام نانو اوكسيد الالمنيوم-الماء

حسين طلال ذيبان
مدرس مساعد
هندسة تقنيات التبريد والتكييف - كلية دجلة الجامعة

الخلاصة

تمت عددياً دراسة خواص الجريان وانتقال الحرارة لمائع نانو اوكسيد الالمنيوم-الماء لمدى من عدد رينولدز 3000, 4500, 6000 و 7500 مع مدى من التركيز الحجمي للدقائق من 1%, 2%, 3% و 4%. يتألف جهاز الاختبار من دورة باردة ودورة حارة مع جريان متعاكس للمائع داخل انبوب مزدوج متحد المركز بطول متر واحد. الانبوب الداخلي مصنوع من النحاس الاملس بقطر يعادل 15 مليمتر. والأنبوب الخارجي مصنوع من النحاس الاملس بقطر يعادل 50 مليمتر. جريان المائع الساخن خلال الانبوب الخارجي وجريان المائع البارد (او النانوي) خلال الانبوب الداخلي. الشروط الحدودية لهذه الدراسة هي السطح الخارجي معزول مع سرع متغيرة (0.2, 0.3 , 0.4 و 0.5)م\ثا للدورة الباردة وسرعة ثابتة (0.5)م\ثا للدورة الساخنة.

النتائج تبين ان معامل انتقال الحرارة وعدد نسيلت تزداد بزيادة عدد رينولد ومعامل التركيز الحجمي . والنتائج العددية تمثلت بأعلى نسبة تحسين لعدد نسلت ومعامل انتقال الحرارة ب 9.5% و 13.5% على التوالي عند عدد رينولد 7100 ومعامل التركيز الحجمي للجزيئات 4%.كذلك

النتائج بينت توافق جيد مع معادلة عددية عند معامل التركيزالحجمي للجزيئات 1%, 2% و 3% ولكن بمعامل الكسر الحجمي 4% حدث اختلاف بسيط .

1. INTRODUCTION

Rapid development in all sectors, which is infrastructure, industrial, transportation, defense, space; managing high thermal loads has become very critical. For that reason, several cooling technologies have been researched. However, the conventional technique of heat transfer by means of a flow system including fluids like water, ethylene glycol, mineral oils has always been popular and would always remain popular due to its simple nature. Conventional heat transfer systems used in applications like petrochemical, refining, and power generation are rather large and involve significant amount of heat transfer. However, in certain applications like electronics cooling in laptops and microprocessors, engine cooling in automobiles, cooling in power electronics used in military devices, cooling in space applications and many other areas, small heat transfer systems are required. These applications have a critical relationship between size of a mechanical system and the cost associated with manufacturing and operation. If improvements could be made in the existing heat transfer systems such as enhancing the performance of the heat transfer fluid, a lesser heat exchanger surface area and hence, a lesser space would be required to handle a specified amount of cooling load. The situation would lead to smaller heat transfer systems with lower capital costs and higher energy efficiencies. In this pursuit, numerous researchers have been investigating better techniques to enhance the thermal performance of heat transfer fluids. One of the methods used is to add nano-sized particles of highly thermally conductive materials like carbon, metal, metal oxides into the heat transfer fluid to improve the overall thermal conductivity of the fluid. The dispersion or suspension thus obtained is called nanofluid.

With the recent improvements in nanotechnology, the production of particles with sizes on the order of nanometers (nanoparticles) can be achieved with relative ease. Nanofluid (nanoparticles fluid suspensions) is the term coined by, **Choi,1995** to describe this new class of nanotechnology based heat transfer fluids that exhibit thermal properties superior to those of their host fluids or conventional particle fluid suspension. As a consequence, the idea of suspending these nanoparticles in a base liquid for improving thermal conductivity has been proposed recently,**Masuda, et al., 1993.**

2. HEAT TRANCFER ENHANCEMENT WITH NANOFLUIDS

A number of numerical and experimental studies were conducted to examine the effect of Al_2O_3-water nanofluids on heat exchanger enhancement under the laminar and turbulent regime. The configurations of heat transfer devices that were examined include concentric tube heat exchanger, some with twist and spiraled rod inserts, shell and tube heat exchanger, multichannel heat exchangers for electronic chip cooling.

Increase in the thermal conductivity of the working fluid improves the efficiency of the associated heat transfer process. When forced convection in tubes is considered, it is expected that heat transfer coefficient enhancement obtained by using a nanofluid is equal to the enhancement in thermal conductivity of the nanofluid, due to the definition of Nusselt number. However, research into the convective heat transfer of nanofluids indicates that the enhancement of heat transfer coefficient exceeds the thermal conductivity enhancement of nanofluids **,Hwang, 2009** and **Heris, 2006 and 2007.**

Pak and Cho, 1998, studied experimentally the heat transfer of Al_2O_3-water nanofluid at turbulent flow when detail of heat exchanger and the boundary conditions were circular pipe D=10.66 mm and length L=4.8 m at constant heat flux. At range of Reynolds number Re $=10^4 - 10^5$ and particle concentration (φ): 1.34%, 2.78% and 4.33% by volume. They found that the Nusselt number of the dispersed fluids for fully developed flow increased by increasing volume concentration as well as with Reynolds number. Also found that

maximum enhancement of heat transfer coefficient was 12% smallest than that in pure water at 3% particle concentration.

Fotukian and Esfahany, 2010, studied experimentally the turbulent flow of nanofluids with different volume concentrations (φ = 0.03%, 0.054%, 0.067% and 0.135% by volume) of nano particles flowing through shell and tube heat exchanger at constant wall temperature with range of Reynolds number from 6×10^4 to 3.1×10^4. Results had clearly showed a decrease in a the ratio of heat transfer coefficient of nanofluid with Reynolds number compared to that of pure water by 48% at φ = 0.054%.

Vasu et al., 2007, developed an empirical correlation for the thermal conductivity of Al_2O_3/water and Cu/water nanofluids, considering the effects of temperature, volume fraction and size of the nano particle. A correlation for the evaluation of Nusselt number was also developed, presented, and compared in graphical form. This enhanced thermo physical and heat transfer characteristics made fluids embedded with nano materials as excellent candidates for future applications.

Huminic and Huminic, 2011, used a three-dimensional analysis to study the heat transfer characteristics of a double-tube helical heat exchangers using nanofluids under laminar flow conditions. CuO and TiO_2 nanoparticles with diameters of (24 nm) dispersed in water with volume concentrations of (0.5–3 vol. %) were used as the working fluid. The mass flow rate of the nanofluid from the inner tube was kept and the mass flow rate of the water from the annulus was set at either half, full, or double the value. Effects of nanoparticles concentration level and of the Dean number on the heat transfer rates and heat transfer coefficients were presented. The results showed that for 2% CuO nanoparticles in water and same mass flow rate in inner tube and annulus, the heat transfer rate of the nanofluid is approximately (14%) greater than of pure water. The results also showed that the convective heat transfer coefficients of the nanofluids and water increases with increasing of the mass flow rate and with the Dean number.

Khalifa and Banwan, 2015, studied experimentally the effect of nanofluids with different volume concentrations (φ = 0.25%, 0.5%, 0.75% and 1% by volume) on heat transfer under turbulent regime in double concentric tube heat exchanger for four different volumetric flow rates of 150, 200, 250 and 300 L/h. Results showed the convective heat transfer increase by increasing particle concentration and flow rare. The maximum enhancement obtained in Nusselt number and heat transfer coefficient was 20 and 22.8% respectively, at Reynolds number6026 and particle concentration of 1%.

Nguyen et al., 2007, studied experimentally the investigation on turbulent heat transfer in closed system for cooling of microprocessors with Al_2O_3 nanofluids at particle concentration (φ) 1%, 3.1% and 6.8% by volume. The Reynolds numbers range that used in this study from 3×10^3 to 15×10^3. He concluded that the inclusion of nanoparticles into water produced a considerable enhancement of the cooling block convective heat transfer coefficient. Results showed the maximum enhancement in heat transfer coefficient was 40% at φ =6.8%.

Vajjha et al., 2010, investigated experimentally the heat transfer of Al_2O_3water nanofluid at turbulent flow. The detail of heat exchanger and the boundary conditions was circular pipe D=3.14 mm and length L=1.168 m at constant heat flux. The range of Reynolds number (Re) that used $3 \times 10^3 - 1.6 \times 10^4$, the particle concentration 2%, 4%, 6%, 8% and 10% by volume. The results showed that by increasing the volume concentration, the wall shear stress and heat transfer rates increase also it showed the maximum enhancement of heat transfer coefficient was 81.74% at φ = 10% and Re = 7240.

The objectives of the study presented in this paper are to present the effect of heat transfer enhancement with and without Al_2O_3/water and comparison with other researches in a double-pipe heat exchanger.

3. HEAT EXCHANGER CONFIGURATION

The geometry consists of a three-dimensional counter flow double pipe heat exchanger with length equal to (l m). The outer diameter of the heat exchanger is equal to (50 mm) and the inner diameter of the heat exchanger is equal to (15 mm). The outer wall of heat exchanger is thermally insulated. The nanofluid enters the inner diameter (cold loop) with uniform velocity at (0.2, 0.3, 0.4 and 0.5 m/s) and temperature at (300 K). The velocity at hot loop of the outer diameter is constant at (0.5 m/s) with temperature at (350 K). The geometry is shown in **Fig. 1.**

4. THERMOPHYSICAL PRPPERTIES OF NANOFLUID

The calculation of nanofluid thermo physical properties is a crucial point since the results are strongly affected by them. As previously mentioned, the determination of nanofluids thermo physical properties is a very active area of research. The use of classical models is not certain for nanofluids, but, on the other hand, scarce experimental data on nanofluids are available to allow us to select a single model.

The physical properties of the nanofluid used in this work are calculated using the standard equations. **,Eastman, et al., 2001.**

The density (ρ_{nf}) in kg/m³is determined by the following equation

$$\rho_{nf} = \varphi \cdot \rho_p + (1-\varphi) \cdot \rho_{bf} \quad (1)$$

The specific heat $\left(C_{p_{nf}}\right)$in kJ/kg K is determined by the following equation

$$C_{p_{nf}} = (1-\varphi) Cp_{bf} + \varphi \cdot Cp_p \quad (2)$$

The following equation is used to calculate the viscosity ratio (μ_r)

$$\mu_r = \frac{\mu_{nf}}{\mu_{bf}} = 123\varphi^2 + 7.3\varphi + 1 \quad (3)$$

The thermal conductivity ratio (k_r) is calculated from

$$k_r = \frac{k_{nf}}{k_{bf}} = 4.97\varphi^2 + 2.27\varphi + 1 \quad (4)$$

Therefore, in our simulations the properties of nanofluids are temperature-dependent. Table 1.shows the properties of nanofluids at the inlet of internal pipe.

5. MATHEMATICAL CALCULATIONS

In the present study, the γ-Al_2O_3 nanoparticles dispersed in DI water were used to investigate the convective heat transfer coefficient and Nusselt number of the nanofluids. Thus, it can be calculated from the following equations:

The heat transfer rate into the cooling water $(Q_c)$is defined as:

$$Q_{bf} = \dot{m}_{bf} C_p \Delta T_{bf} \quad (5)$$

The heat transfer rate into the nanofluid$(Q_{nf})$is defined as:

$$Q_{nf} = \dot{m}_{nf} \cdot C_{p_{nf}} \Delta T_{nf} \quad (6)$$

The heat transfer coefficient (h) and the Nusselt number (Nu) of the cooling water are computed from the following equations:

$$h = \frac{Q_w}{A_S(T_W - T_f)} \quad (7)$$

$$Nu = \frac{hD}{k} \quad (8)$$

where $T_f = \frac{T_{in}+T_{out}}{2}$ (9)

The mathematical heat transfer coefficient $(h_{nf})$and Nusselt number of the nanofluid(Nu_{nf})are computed from the following equations:

$$h_{nf} = \frac{Q_{nf}}{A_s(T_w - T_{f,nf})} \quad (10)$$

$$Nu_{nf} = \frac{h_{nf}D}{k_{nf}} \quad (11)$$

The Reynolds number of cooling water (Re) and nanofluid (Re_{nf}) are obtained by the following equations:

$$Re = \frac{\rho_c v_c D_i}{\mu_w} \quad (12)$$

$$Re_{nf} = \frac{\rho_{nf} v_c D_i}{\mu_{nf}} \quad (13)$$

6. GOVERNING EGUATIONS

The basic equations that describe the flow and heat are conservation of mass, momentum and energy equations. These equations describe two-dimensional, turbulent and incompressible flow takes which the following forms, **Arnal, 1982.**

The assumptions that used for the instantaneous equation are:-

1- Steady, two-dimensional, incompressible flow, single phase flow, non-viscous, no slip, irrotational.
2- Cylindrical coordinate.
3- Thermal equilibrium between the nanoparticles and base fluid.

(i)*Conservation of Mass*

$$\frac{\partial}{\partial z}(\rho u) + \frac{1}{r}\frac{\partial}{\partial r}(\rho r v) = 0 \quad (14)$$

(ii) *Momentum Equations*

u-momentum (z-direction)

$$\frac{1}{r}[\frac{\partial}{\partial z}(\rho ruu)+\frac{\partial}{\partial r}(\rho ruv)]=-\frac{\partial p}{\partial z}+\frac{1}{r}[\frac{\partial}{\partial z}(r\mu_{eff}\frac{\partial u}{\partial z})+\frac{\partial}{\partial r}(r\mu_{eff}\frac{\partial u}{\partial r})]+S_u \quad (15)$$

vv-momentum (r-direction)

$$\frac{1}{r}[\frac{\partial}{\partial z}(\rho ruv)+\frac{\partial}{\partial r}(\rho rvv)]=-\frac{\partial p}{\partial r}+\frac{1}{r}[\frac{\partial}{\partial z}(r\mu_{eff}\frac{\partial v}{\partial z})+\frac{\partial}{\partial r}(r\mu_{eff}\frac{\partial v}{\partial r})-\Gamma^v\frac{v}{r^2}]+S_v \quad (16)$$

(iii) *Energy Equation*

$$\frac{1}{r}[\frac{\partial}{\partial z}(\rho ruT)+\frac{\partial}{\partial r}(\rho rvT)]=\frac{1}{r}[\frac{\partial}{\partial z}(r\Gamma_{eff}\frac{\partial T}{\partial z})+\frac{\partial}{\partial r}(r\Gamma_{eff}\frac{\partial T}{\partial r})] \quad (17)$$

The turbulence model utilized in this analysis is the two equation k-Epsilon model. This model is utilized for its proven accuracy in heat exchanger analysis and for its applicability to confined fluid flow. (k- ε) Turbulence Model is one of the most widely used turbulence models is the two-equation model of kinetic energy (k) and its dissipation rate (**ε**). The turbulence according to, **Launder and Spalding, 1972** is assumed to be characterized by its kinetic energy and dissipation rate (**ε**), where

(i) *Turbulence Energy, k*

$$\frac{1}{r}[\frac{\partial}{\partial z}(\rho ruk)+\frac{\partial}{\partial r}(\rho rvk)]=\frac{1}{r}[\frac{\partial}{\partial z}(r\Gamma^k\frac{\partial k}{\partial z})+\frac{\partial}{\partial r}(r\Gamma^k\frac{\partial k}{\partial r})]+G-\rho\varepsilon \quad (18)$$

(ii) *Energy Dissipation Rate, ε*

$$\frac{1}{r}[\frac{\partial}{\partial z}(\rho ru\varepsilon)+\frac{\partial}{\partial r}(\rho rv\varepsilon)]=\frac{1}{r}[\frac{\partial}{\partial z}(r\Gamma^\varepsilon\frac{\partial \varepsilon}{\partial z})+\frac{\partial}{\partial r}(r\Gamma^\varepsilon\frac{\partial \varepsilon}{\partial r})]+c_1\frac{\varepsilon}{k}G-c_2\rho\frac{\varepsilon^2}{k} \quad (19)$$

where

$$G=\mu_t\{2[(\frac{\partial u}{\partial z})^2+(\frac{\partial v}{\partial r})^2+(\frac{v}{r})^2]+(\frac{\partial u}{\partial z}+\frac{\partial v}{\partial r})^2\}+S_G \quad (20)$$

S_G given by**, Ideriah,1975**.

$$S_G=-\frac{2}{3}\mu_t\left[\frac{\partial u}{\partial z}+\frac{\partial v}{\partial r}\right]^2-\frac{2}{3}\rho k\left[\frac{\partial u}{\partial z}+\frac{\partial v}{\partial r}\right] \quad (21)$$

Also, $\mu_t=\rho c_\mu k^2/\varepsilon$ (22)

The values of the empirical constant used here are given in **Table 2**, **Launder and Spalding,1974.**

7. COMPUTATIONAL METHODOLOGY

Computational fluid dynamics (CFD) simulation is performed to analysis the heat transfer in heat exchanger. A commercially available CFD code**, Fluent 6.3.26, 2009,** was used to perform all simulations. Fluent is a pressure based flow solver that can be used with structured or unstructured grids. An unstructured grid was used for the study. Solutions were obtained by numerically solving the Navier-Stokes and energy equation through a control volume technique. All geometric construction and meshing were performed with (GAMBIT v2.4.6) program.

The meshing of the three-dimensional model starts with the completion of the geometric construction and assembly by using gambit program. During the building of these models it is critical to take into account the unique geometry and post-processing that will occur after a solution is obtained in fluent program, as this can significantly influence how a model is put together. Model construction, assembly and meshing require a trial and error approach that many times needs multiple iterations before a good geometry and mesh can be developed. Generally, the geometry is created from the ground up meaning that points are placed in the model with lines being drawn between points. Faces are made from lines and finally volumes emerge from the assembly of faces. **Fig. 2**shows the mesh of the test rigs of heat exchanger at tetrahedral cells.

Pressure and velocity were coupled with the Semi-Implicit Method for Pressure Linked Equations (SIMPLE) algorithm. SIMPLE uses a relationship between velocity and pressure corrections to obtain mass conservation and a pressure field.

Before starting any computations Fluent requires the flow to be initialized based on some condition within the model. This initialization process acts as an initial guess to the solution flow field. For all computational simulations the flow field is initialized by the inlet conditions of the cold water to start run the model.

Several times a solution could not be obtained due to the inability of the residual values to converge to an appropriate level. In cases where this issue is prevalent it is possible to adjust under-relaxation factors. The segregated solver uses under-relaxation to control the update of computed variables at iterations. Default values are generally set by Fluent to meet the demands of the widest range of flow scenarios. Unfortunately, these values do not always provide converged residual values for the models being investigated, so they are changed from their defaults values of 0.3, 0.7, 1.0, 0.8, 0.8 and 1.0 for pressure, momentum, energy, turbulent kinetic energy, turbulent dissipation rate and viscosity, respectively, to 0.2, 0.5, 0.8, 0.5, 0.5 and 0.9.

Solution convergence means that the results are essentially constant from iteration to iteration, and verifying this is a critical step to achieving accurate results. Convergence is declared on the basis of the following strict criteria: (i) global mass and energy imbalances drop below 0.01%; (ii) the flow field is unchanging, based on observation of profiles of velocity, pressure, temperature, and turbulence quantities in critical areas. There is no exact rule for determining when a solution is complete.

Fluent has defaults values of convergence set to (10^{-3}) for all quantities except energy, which is set to (10^{-6}). During this study the residuals were required to drop to values of (10^{-4}), with the exception of energy, which was required to reach (10^{-7}). **Fig. 3**shows scaled residuals of continuity, momentum, energy, k and ε as the solution progresses to convergence around 2500 iterations to reach the specified convergence levels.

8. RESULTS AND DISCUSSION

The nanopowder γ-Al_2O_3 with a base fluid of DI water with four different particles volume fractions of 1%, 2%, 3% and 4% and four different velocities of 0.2, 0.3, 0.4 and 0.5 (m/s) under turbulent flow regime were investigated in concentric counter flow heat exchanger to study the heat transfer enhancement due to nanofluids.

Before initiating systematic numerical on nanofluids, the reliability and accuracy of numerical measurements, were tested using DI water alone. Numerical results were compared with the prediction of Dittus-Boelter correlation, **Incropera and DeWitt, 2009,** shown below.

$$Nu = 0.023 Re^{0.8} Pr^{n}$$

for $1.5 \leq Pr \leq 500$; $10^4 \leq Re \leq 10^6$ (23)

where n = 0.4 for heating.

Fig. 4 displays the calculated Nusselt number for pure water at various Reynolds numbers that compared with the equation given by Dittus–Boelter and found bad agreement because the high Reynolds number that deals with this correlation above 10^4. (The conditions in present study resemble at the conditions in the equation 23), but when compared with Gnielinski equation, **Bejan, 1993.**

$$\left.\begin{aligned} &Nu = 0.012\,(Re^{0.87} - 280)\,Pr^{0.4} \\ &\text{for } 7 \le Pr \le 500;\ 3*10^3 \le Re \le 10^6 \end{aligned}\right\} \quad (24)$$

As it is shown an excellent agreement is observed with maximum deviation and average deviation of computed values from theoretical equation being 9 and 2%, respectively, over the range of the Reynolds numbers studied. This correlation given by Gnielinski equation over the traditional Dittus–Boelter equation, because the errors are usually limited to about ±10%. Also the last point in fluent shows higher than in Gnielinski, equation over 7000 Reynolds numbers because the higher separation flow at the velocity exit.

Fig. 5 indicates the comparison between the Nusselt number of nanofluids at four different particles volume fractions and four different volume flow rates at Reynolds number in the range 3000 and 7500 with that of DI water. The numerical results indicate that the Nusselt number of nanofluid is increased by increasing both the Reynolds number and particles volume fraction.

At 1% volume fraction, the Nusselt number is increased from 19.6 to 64.32 by increasing Reynolds number from 3000 to 7500, which are higher than those obtained for DI water alone by 1% and 10.5% respectively. At 2% volume fraction, the Nusselt number is increased from 19.65 to 65.2 by increasing the Reynolds number from 3000 to 7500, which are higher than those obtained for DI water alone by about 3% and 12.3%. For 3% volume fraction the Nusselt number increased from 20.576 to 66.2 by increasing Reynolds number from 3000 to 7000, these values are higher than the values of DI water by 5% and 15.3% respectively. At particles volume fraction of 4% the Nusselt number increased from 20.63 to 67.3 by increasing Reynolds number from 2800 to 7100, these values are higher than the values of DI water by 8.5% and 23.5% respectively.

Fig.6 indicates the contours of temperature distribution along the inner tube of cold flow at Reynolds number 6000 of pure water. This figure shows increasing in temperatures when the fluid moved toward the exit to record higher temperatures at the end tube (cold exit) when the hot flow input at high temperature.

Fig.7 illustrates the dimensionless Nu that presented by calculating the ratio (Nu_{nf}/Nu_w) at different volume fraction that increased from 1% to 4%, and different Reynolds numbers. The dimensionless Nu is at φ = 1% is found to increase from 1.0125 to 1.09 by increasing the Reynolds number from 3000 to 7500. For φ = 2% the dimensionless Nu value is 1.02 to 1.1 at Reynolds number of 3000 and 7500 respectively. Also at φ = 3%, the dimensionless Nu value is increased from 1.033 to 1.105 at Reynolds numbers of 3000 and 7500 respectively. At the highest particle volume fraction used of 4%, the dimensionless Nu is increased from 1.045 to 1.125 when the Reynolds number is increased from 3000 to 7500.

Fig.8 displays the comparison between heat transfer coefficient of DI water and nanofluid for four different particle volume fractions at varies Reynolds numbers. The fluent results indicate that the heat transfer coefficient is increased by increasing both the Reynolds number and particles volume fraction. The heat transfer coefficient (HTC) at φ = 1% is found to increase from 801.5 to 2645.3 by increasing the Reynolds number from 3000 to 7500. For φ = 2% the HTC value are 830.4 and 2723 at Reynolds number of 3000 and 7500 respectively. At φ = 3%, the HTC values are 896.77 and 2847.7 at Reynolds numbers of 3000 and 7500 respectively. At the highest particle volume fraction used of 4%, the HTC is increased from 912.6 to 2990 when the Reynolds number is increased from 3000 to 7500. Therefore, a better heat transfer is achieved and hence the relative gain in heat transfer is higher at lower Reynolds number for a fixed concentration.

The numerical values of Nusselt number with different particle volume fractions and Reynolds numbers are compared with empirical correlation, **Vajjha, et al., 2010,** that presented in **Fig.9.** The boundary conditions, Reynolds number range, base fluid and particles material for the correlation used in the comparison are given in **Table 3**.

$$Nu_{nf} = 0.065\left(Re_{nf}^{0.65} - 60.22\right)(1 + 0.0169\,\varphi^{0.15})Pr_{nf}^{0.542} \quad (25)$$

Fig.9 shows the comparison in particle volume fractions of 1%, 2%, 3% and 4% respectively. The numerical results show a good agreement with, **Vajjha et al., 2010,** correlation at volume fractions of 1%, 2% and 3% as shown in **Fig.9**. The deviation is found to increase with increasing Reynolds number. However, at volume fractions of 4%, the deviation is increased, which may be caused by several effects such as different in configuration of the test section and boundary condition.

9. CONCLUSION

In this study, the flow and heat transfer characteristics of Al_2O_3-water nanofluids for a range of the Reynolds number (3000 to 7500) with a range of volume concentration (1 to 4%) are studied numerically.

- The results show that both the Nusselt number and the heat transfer coefficient of nanofluid are strongly dependent on nanoparticles and increase by increasing of the volume concentration of nanoparticles.
- A good agreement is obtained between the numerical data for water and the results obtained from Gnielinski correlation with a maximum deviation of about 3%.
- The heat transfer coefficient and Nusselt number are increased by increasing Reynolds number.
- Numerical results indicate that the minimum enhancement in Nusselt number and heat transfer coefficient are 1.5% and 4% respectively at Reynolds number of 3000 and particles volume fraction of 1%.
- Numerical results indicate that the maximum enhancement in Nusselt number and heat transfer coefficient are 9.5% and 13.5% respectively at Reynolds number of 7500 and particles volume fraction of 4%.
- These results are in good agreement with correlation of, **Vajjha et al., 2010.**

REFERENCES

- Arnal, M.P., 1982, *A General Computer Program for Two-Dimensional, Turbulent, Re-Circulating Flows*, report No.Fm-83-2.
- Bejan, 1993, Heat Transfer, text book, John Wiley & Sons, New Jersey.
- Choi, S. U. S.,1995, *Enhancing Thermal Conductivity of Fluids with Nanoparticles*, Developments and Applications of Non-Newtonian Flows, The American Society of Mechanical Engineers, New York, FED-Vol. 231 / MD-Vol.66, pp. 99-105.
- Eastman, J. A., Choi, S., Li, S., Yu, W., and Thompson, L. J., 2001, *Anomalously Increased Effective Thermal Conductivities of Ethylene Glycol-Based Nanofluids Containing Copper Nanoparticles*, Appl. Phys. Lett.,Vol. 78(6), pp. 718-720.
- Fotukian, S. M., and Esfahany, M. N., 2010, *Experimental Investigation of Turbulent Convective Heat Transfer of Dilute γ-Al_2O_3/water Nanofluids Inside a Circular Tube*, International Journal of Heat and Fluid Flow; Vol. 31, pp. 606–612.

- Fluent Inc., 2009, *Fluent User's Guide, Version 6.3.26.*
- Hwang, K. S., Jang, S. P., and Choi, S. U. S.2009, *Flow and Convective Heat Transfer Characteristics of Water-Based Al_2O_3Nanofluids in Fully Developed Laminar Flow Regime*, Int. J. Heat Mass Tran., Vol. 52(1-2), pp. 193-199.
- Heris, S. Z., Etemad, S., and Esfahany, M. N., 2006, *Experimental Investigation of Oxide Nanofluids Laminar Flow Convective Heat Transfer*, Int. Commun. Heat Mass, Vol. 33(4), pp. 529-535.
- Heris, S. Z., Esfahany, M. N., and Etemad, S.,2007,*Experimental Investigation of Convective Heat Transfer of Al_2O_3/Water Nanofluid in Circular Tube*, Int. J. Heat Fluid Fl., Vol. 28(2), pp. 203-210.
- Huminic, G., and Huminic, A., 2011,*Heat Transfer Characteristics in Double Tube Helical Heat Exchangers Using Nanofluids*, Int. J. Heat Mass Tran., Vol. 54, pp. 4280–4287.
- Ideriah, F. J. K., 1975, *Review of Equation Solved in TEACH*, private communication.
- Incropera, F.P., and DeWitt, D.P., 2009, *Fundamentals of Heat and Mass Transfer*, text book, Springer.
- Khalifa, A. J. N, and Banwan, M. A., 2015, *Effect of Volume Fraction of γ-Al_2O_3Nanofluid on Heat Transfer Enhancement in a Concentric Tube Heat Exchanger*, Taylor and Francis group, heat transfer engineering, Vol. 36(16), pp. 1387-1396.
- Launder, B.E. and Spalding, D.B., 1972, *Mathematical models of turbulence*, text book, Academic press, London.
- Masuda, H., Ebata, A., Teramae, K., and Hishinuma, N., 1993, *Alteration of Thermal Conductivity and Viscosity of Liquid by Dispersing Ultra-Fine Particles (Dispersion of γ-Al_2O_3, SiO_2, and TiO_2Ultra-Fine Particles)*,NetsuBussei, Vol. 4(4), pp. 227-233.
- Nguyen, C. T., Roy, G., Gauthier, C., and Galanis, N.,2007, *Heat Transfer Enhancement Using Al_2O_3 –Water Nanofluid, for an Electronic Liquid /cooling System*, Applied Thermal Engineering, Vol. 27, pp. 1501-1506.
- Pak, B. C., and Cho, Y. I., 1998, *Hydrodynamic and Heat Transfer Study of Dispersed Fluids with Submicron Metallic Oxide Particles*, Exp. Heat Transfer, Vol. 11(2), pp. 151-170.
- Vajjha, RS., Das, DK., and Kulkarni, DP., 2010, *Development of New Correlations for Convective Heat Transfer and Friction Factor In Turbulent Regime for Nanofluids*, Int. J. Heat Mass Tran., Vol. 53, pp. 4607–4618.
- Vasu, V., Krishna K., and Kumar A.C.S., 2007, *Analytical Prediction of Forced Convective Heat Transfer of Fluids Embedded with Nano Structured Materials (Nanofluids)*, Vol. 69, pp. 411-421.

NOMENCLATURE

Symbol	*Description*	Dimension
A	Area	m^2
As	circumference area (A_s= πDL)	m^2
C_P	spesific heat at constant pressure	kJ/kg.K
P	pressure	Pa
Re	Reynolds number (Re=ρUD/μ)	
Nu	Nusselt number (hd/k)	
T	temperature	˚C
u ,v	velocity component in r, z respectively	m/s
Pr	Prandtl number	
$\dot{m}$	mass flow rate	kg/s
μ_r	viscosity ratio	
K	thermal conductivity	W/m.K
Q	heat transfer rate	W
Γ	diffusion coefficient	N.s / m^2
U_h	velocity at hot loop	m/s
U_c	velocity at cold loop	m/s
T_g	temperature of hot gases	˚C
T_c	temperature at cold loop	˚C
T_h	temperature at hot loop	˚C
r,z	cylindrical coordinate	
L	Length	M
D	diameter	M
Greek Letters		
Φ	particles volume fraction	
ρ	density	kg/m^3
ε	rate of dissipation of kinetic energy	m^2/s^{-3}
μ	viscosity	$N.m/s^2$
Subscript		
nf	Nanofluid	
bf	base fluid (water)	
c	cold flow	
h	hot flow	
f	Film	
w	Wall	
Abbreviation		
DI	de ionized	
HTC	heat transfer coefficient	
SIMPLE	semi-implicit method for pressure linked equation	

Table1. Properties of nanofluids at the inlet of the inner pipe.

Type of fluid	φ(%)	ρ(kg/m3)	μ(Pa.s)*10^{-3}	Cp(J/kg.K)	K_{eff}(W/m.K)	Pr
Pure water	0	998.2	1	4182	0.6	6.5
Al_2O_3/water	1	1027.4	1.02	4046.96	0.617	6.7
Al_2O_3/water	2	1057.2	1.13	3922.46	0.635	7
Al_2O_3/water	3	1086.9	1.26	3804.78	0.653	7.3
Al_2O_3/water	4	1116.6	1.41	3693.36	0.671	7.8

Table2. Values of constants in the (k-ε) model, **Launder and Spalding, 1972.**

C_μ	C_D	C_1	C_2	σ_k	σ_ε
0.09	1.0	1.44	1.92	1.0	1.3

Table3. Nanofluids, boundary conditions and Reynolds range for the correlation used in the comparison, **Vajjha et al., 2010**.

Author	Nanofluids	Conditions	Re range
Vajjha et al.	Cu,SiO_2, Al_2O_3	Turbulent	3000-16000

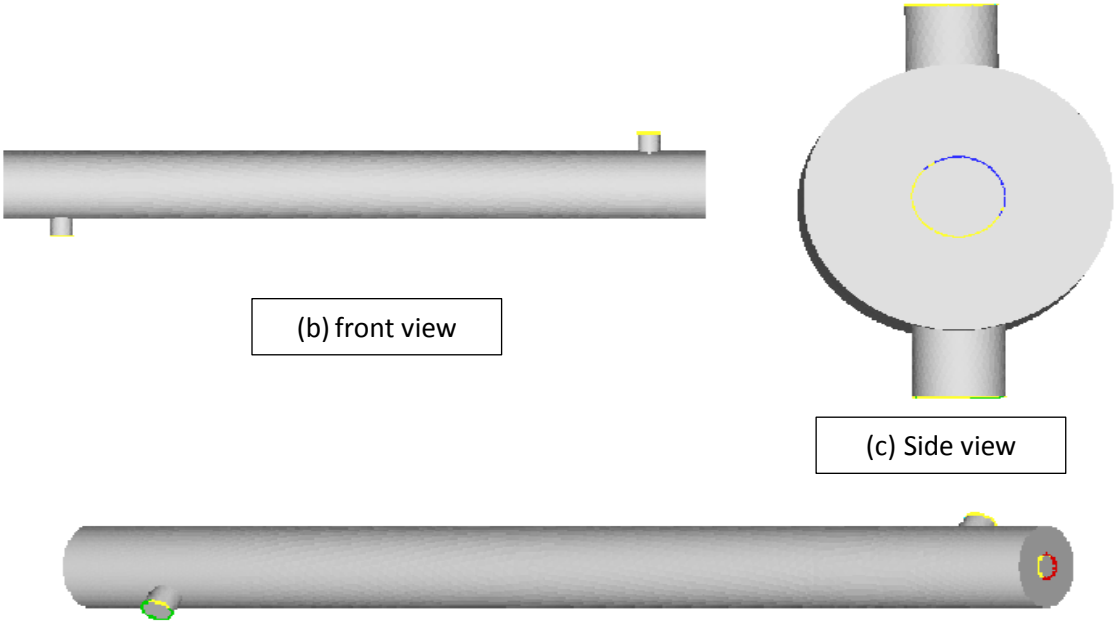

Figure 1. Heat exchanger geometry.

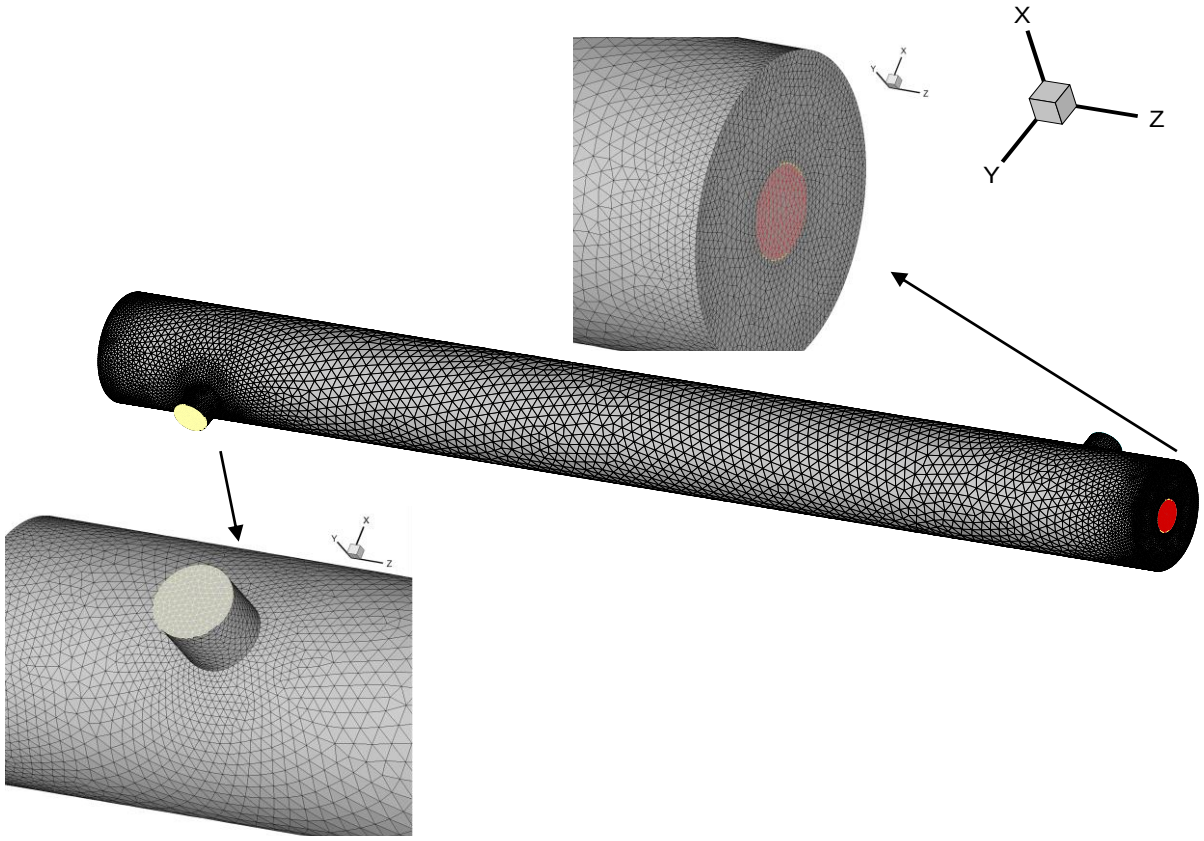

Figure 2. Heat exchanger mesh with tetrahedral cell.

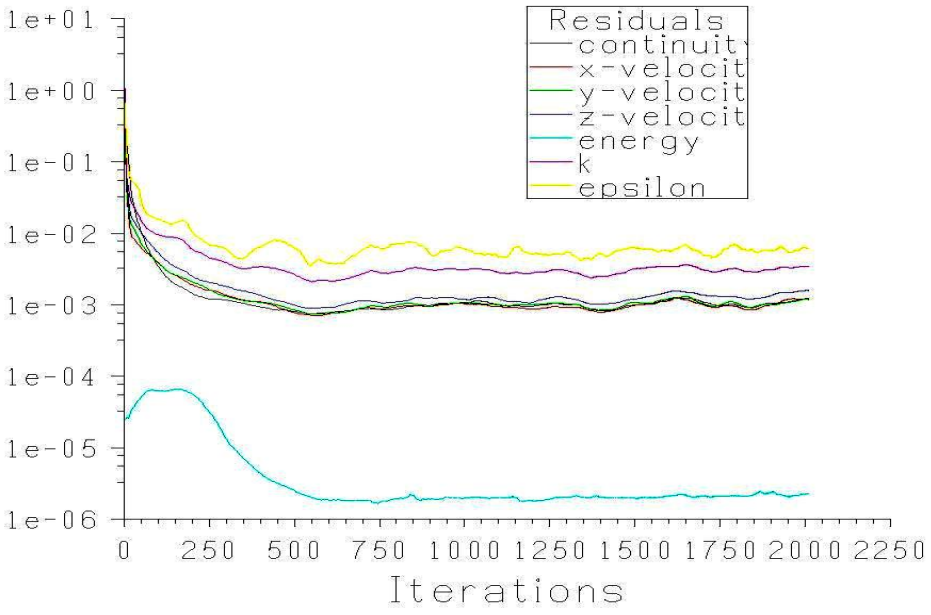

Figure 3. Typical residual convergence for heat exchanger model at Re=6000.

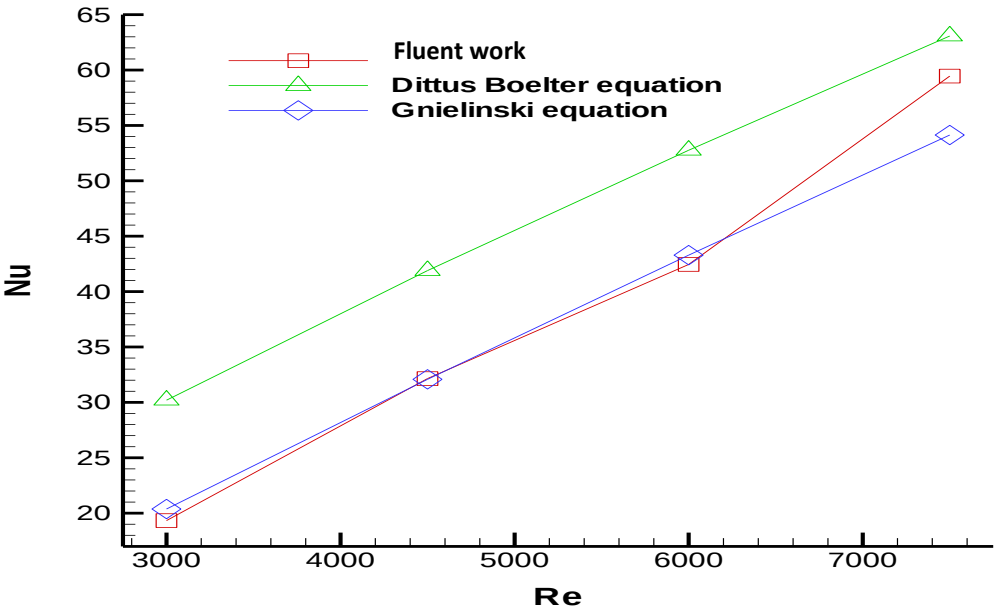

Figure 4. Comparison between the computed values of the Nusselt numbers and the equations given by Gnielinski and Dlttus -Boelterfor water.

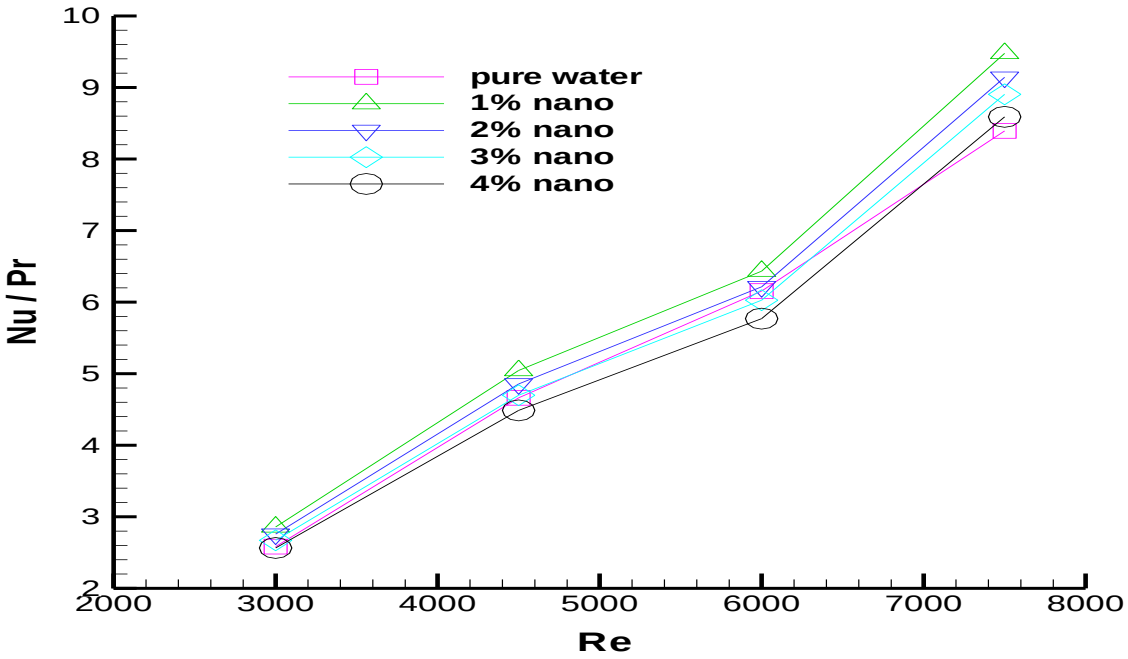

Figure 5. Comparison between dimensionless Nusselt/Prandtl numbers of nanofluids and DI water.

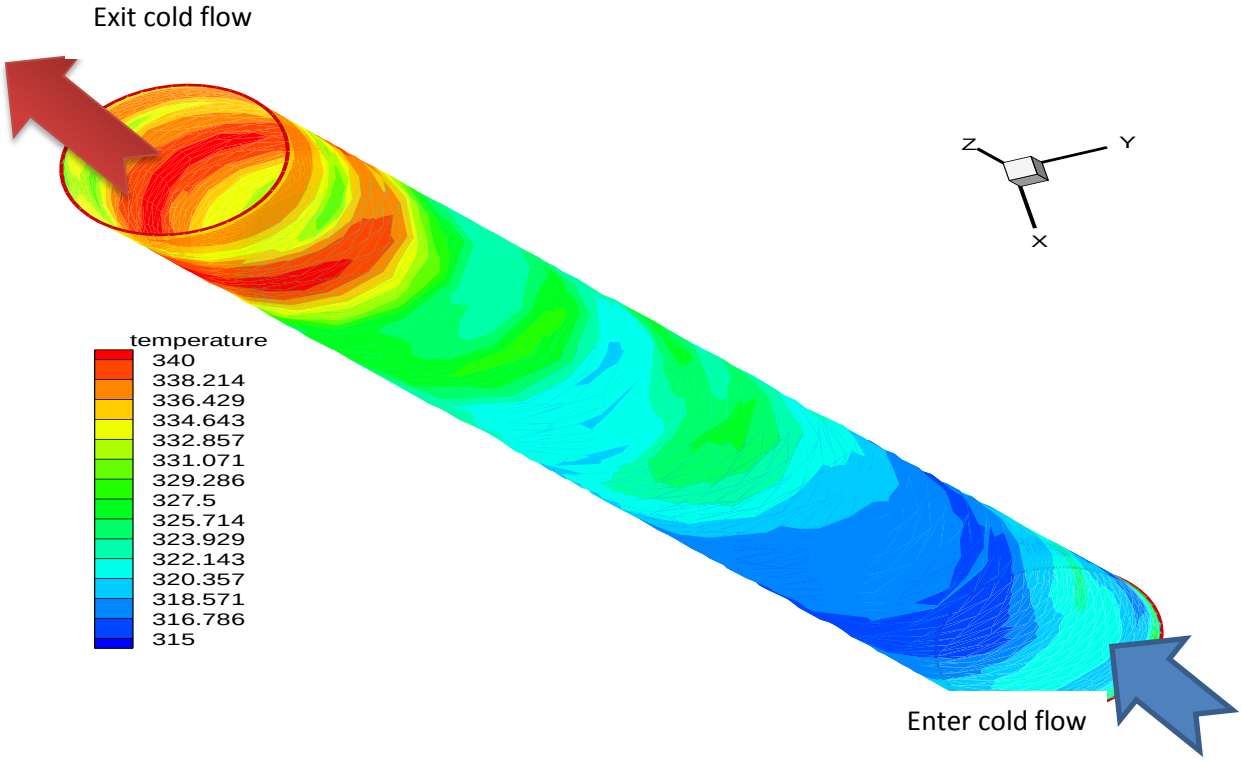

Figure 6. Contours of temperature distribution along the inner tube at Re=6000 of pure water.

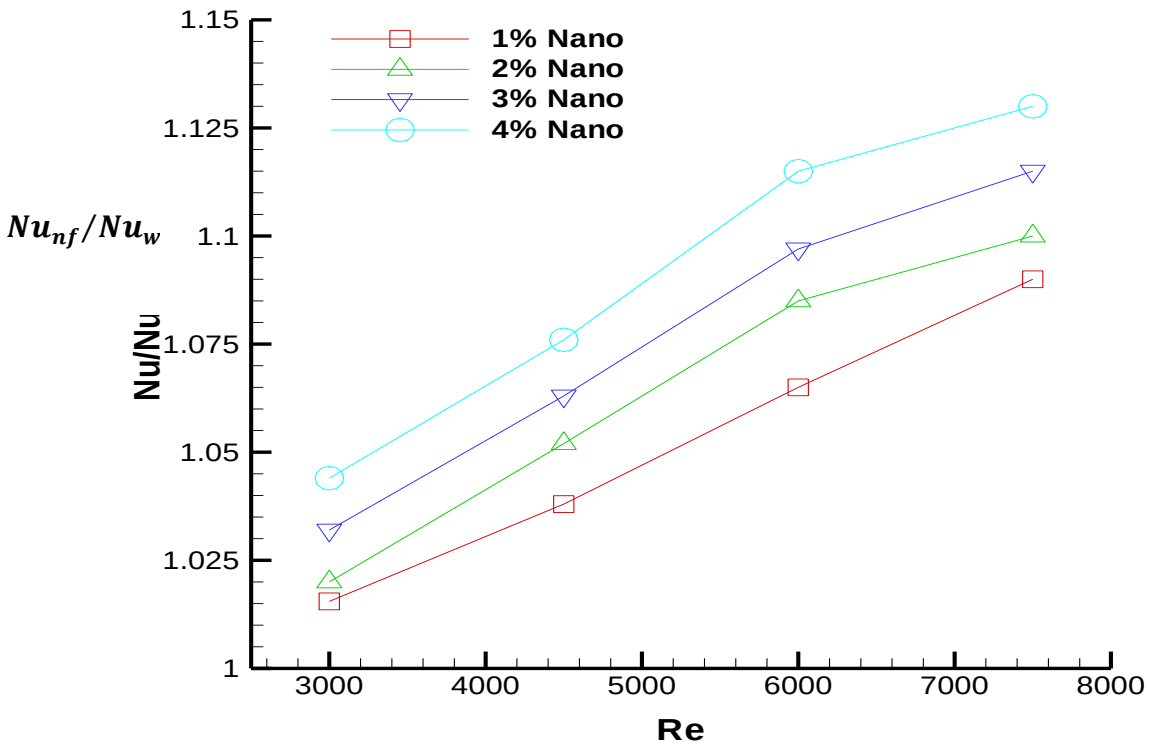

Figure 7. The ratio of (Nu_{nf}/Nu_w) at various Reynolds numbers and particles volume fractions.

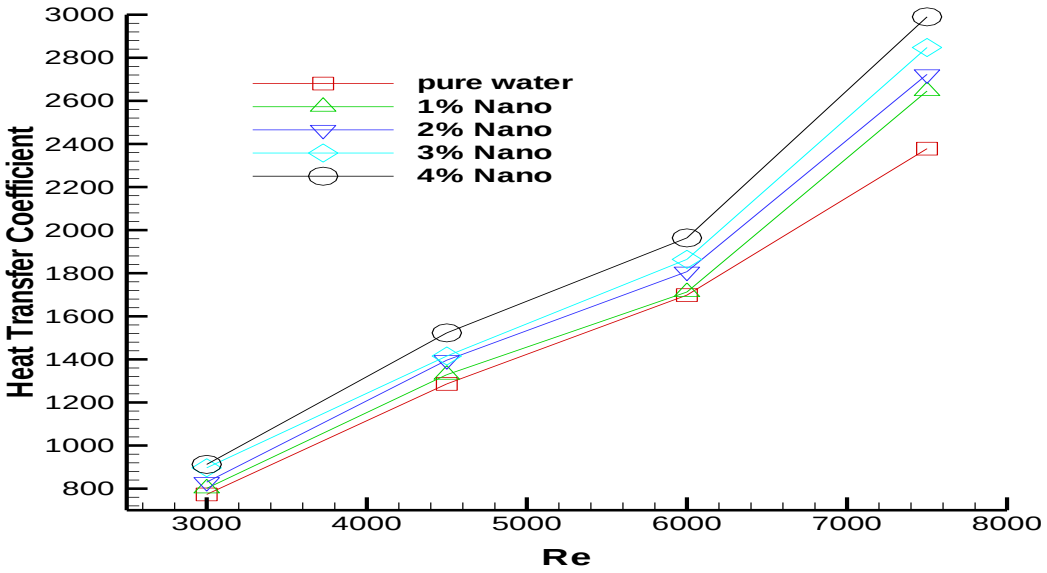

Figure 8. Heat transfer coefficient of nanofluids an DI water at various particles volume fractions and Reynolds numbers.

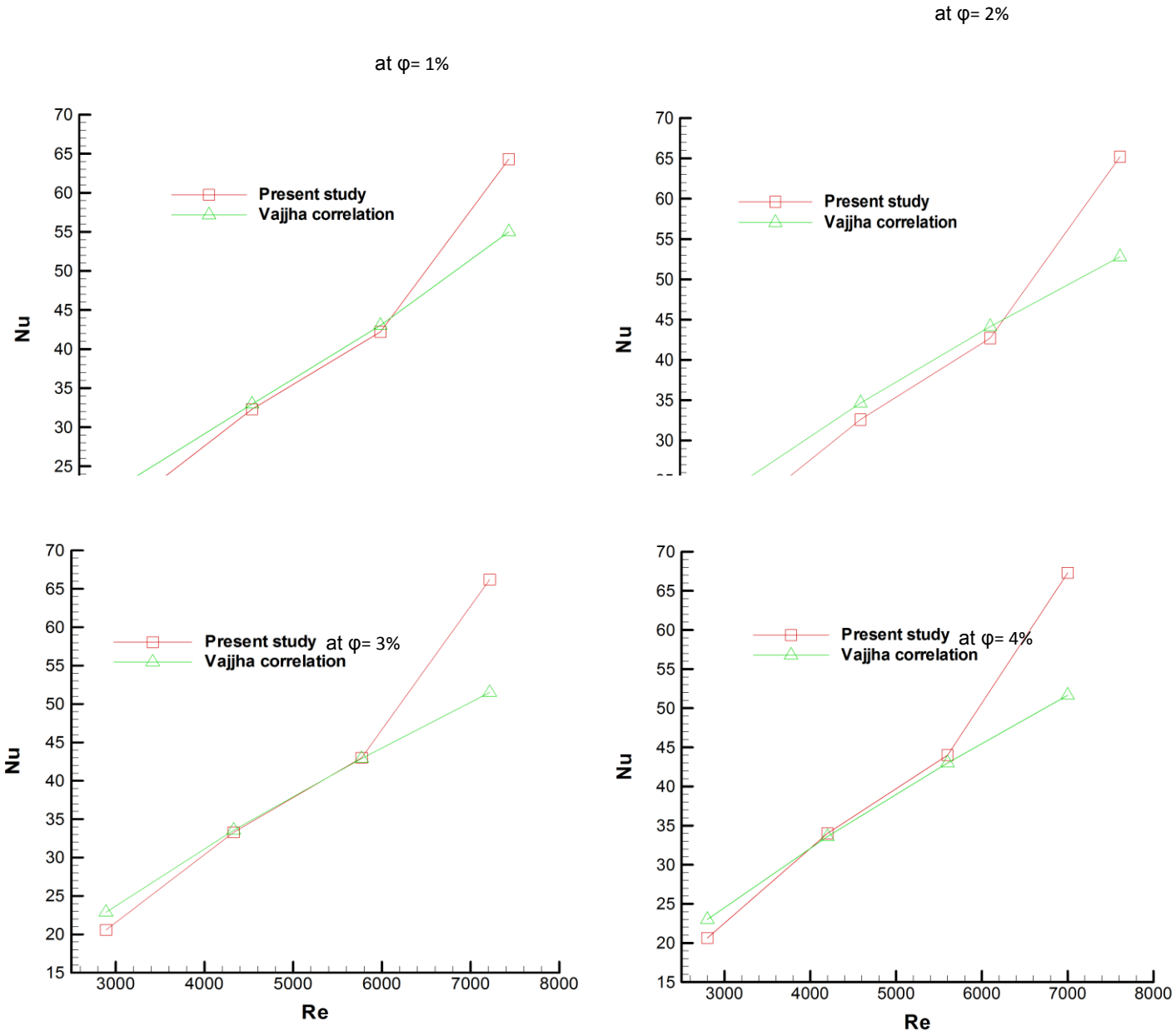

Figure 9. Comparison between present study and empirical correlation forVajjha et al. at volume concentrations 1%, 2%, 3% and 4% of nanofluids.